Sencadas, VJGDS.; Areias Cepa, A.; Areias, A.; Botelho, G.; Fonseca, A.; Neves, I.; Gómez Ribelles, JL.... (2012). Determination of the parameters affecting electrospun chitosan fiber size distribution and morphology. Carbohydrate Polymers. 87(2):1295-1301.

Determination of the parameters affecting electrospun chitosan fiber size distribution and morphology

V. Sencadas[1]; D. M. Correia[2]; A. Areias[1]; G. Botelho[2]; A. M. Fonseca[2]; I. C. Neves[2]; J. L. Gómez-Ribelles[3,4,5] and S. Lanceros-Mendez[1]

[1] *Centro/Departamento de Física, Universidade do Minho, Campus de Gualtar, 4710-058 Braga, Portugal*

[2] *Dept. Química, Centro de Química, Universidade do Minho, Campus de Gualtar, 4710-057 Braga, Portugal;*

[3] *Centro de Biomateriales e Ingeniería Tisular, Universidad Politécnica de Valencia, Camino de Ver s/n, 46022 Valencia, Spain*

[4] *Centro de Investigación Príncipe Felipe, Autopista del Saler 16, 46013 Valencia, Spain*

[5] *CIBER en Bioingeniería, Biomateriales y Nanomedicina, Valencia, Spain*

*e-mail: vsencadas@fisica.uminho.pt

Abstract

The production of chitosan nanofiber mats by electrospinning presents serious difficulties due to the lack of suitable solvents and the strong influence of processing

parameters on the fiber properties. Two are the main problems to be solved: to control the properties of the solution in order to obtain large area uniform fiber mats by having a stable flow rate and to avoid sparks during the process, damaging the fiber mats. In this work chitosan electrospun mats have been prepared form solutions of trifluoroacetic acid / dichloromethane mixtures, allowing to solve the aforementioned problems. Mats with uniform fibers of submicron diameters without beads were obtained. Further, the influence of the different solution and process parameters on the mean fiber diameter and on the width of the distribution of the fiber sizes has been assessed. Solvent composition, needle diameter, applied voltage and traveling distance were the parameters considered in this study.

Introduction

Increasing attention has been given in recent years to natural polymers, such as polysaccharides, due to their abundance in nature, unique structures and characteristics with respect to synthetic polymers (Honarkar & Barikani, 2009). Chitosan is a natural linear polysaccharide composed of glucosamine and N-acetyl glucosamine units linked by β (1-4) glycosidic bonds. Although naturally present in some microorganisms and fungi, commercial chitosan is industrially produced by partial deacetylation of chitin by removal of acetamide groups. Chitin is the second most abundant natural polysaccharide after cellulose. It is mainly found in crustacean shells (shrimp, crab, etc.), insect cuticle and cell walls of fungi (Baldrick, 2010; Fernandez-Megia, Novoa-Carballal, Quiñoá & Riguera, 2005; Krajewska, 2005; Malafaya, Silva & Reis, 2007; Ravi Kumar, 2000). The degree of deacetylation, DD, which defines the distinction between chitin and chitosan, is not precisely established.

The term chitosan is found in the literature to describe polymers of chitosan with different molecular weights, viscosity and degree of deacetylation (40-98 %) (Baldrick, 2010). However, the term chitosan is generally applied when the degree of deacetylation is above 70 % and the term chitin is used when the degree of deacetylation is below 20% (Baldrick, 2010).

Chitosan in its crystalline form is usually insoluble in aqueous solutions above a pH of ~7. However, due to the existence of primary amine groups, the structure can be protonated and the protonate free amine groups on glucosamine facilitate the solubility of the molecule, being therefore highly soluble in acid pH (Pillai, Paul & Sharma, 2009; Yaghobi & Hormozi, 2010).

Chitosan offers many structural possibilities for chemical modifications in order to induce novel properties, functions and applications, in particular in the biomedical area. It is nontoxic, biocompatible and biodegradable and therefore an excellent material for biomedical applications (Jayakumar, Menon, Manzoor, Nair & Tamura, 2010; Jayakumar, Prabaharan, Nair, Tokura, Tamura & Selvamurugan, 2010; Jayakumar, Prabaharan, Sudheesh Kumar, Nair & Tamura, 2011).

Recently, much attention has been paid to chitosan based nanofibers as biomaterial. There are several methods for the fabrication of nanofibers, making use of chemical, thermal and electrostatic principles (Beachley & Wen, 2010). The polymer nanofiber fabrication methods most commonly associated with biomedical applications are electrospinning, self-assembling, peptide reactions and phase separation. The electrospinning process has attracted much attention for the production of polymer fibers as it can produce them with diameters in the range from several micrometers down to tens of nanometers, depending on the polymer and processing conditions (Jayakumar, Prabaharan, Nair & Tamura). The nanofibers produced by this technique

are formed from a liquid polymer solution or melt that is feed through a capillary tube into a region of an electric field generated by connecting a high voltage power source to the capillary tube.

Chitosan nanofibers were successfully prepared by Ohkawa et al. (Ohkawa, Cha, Kim, Nishida & Yamamoto, 2004). The authors studied the solvent effect on the morphology of electrospun chitosan nanofibers by varying chitosan relative concentration with different solvents. The solvents tested were diluted hydrochloric acid, acetic acid, formic acid and trifluoracetic acid (TFA). It was found that when the concentration of chitosan increased, the morphology of the deposited fibers on the collector changed from spherical beads to an interconnected fibrous system. Further, the addition of dichloromethane (DCM) to the chitosan/TFA solution improved the homogeneity of the electrospun chitosan nanofibers. Electrospinning conditions were optimized in order to obtain homogeneous chitosan nanofibers with an average diameter of 330 nm. Other studies on electrospun chitosan nanofibers have been also reported (Jayakumar, Prabaharan, Nair & Tamura). Schiffman et al. obtained bead-free electrospun chitosan nanofibers from a solution of TFA and chitosan with different molecular weights. A small correlation between viscosity and fiber diameter was found (Schiffman & Schauer, 2006, 2007). Despite these efforts, large fiber mats with controlled fiber dimensions are not obtained mainly due to the large electrical conductivity of the TFA solvent, which leads to an unstable process in which the flow rate is controlled by the electric field more than by the dispenser. Further, electrical sparks often occur, damaging parts of the samples. In fact, almost no cell cultures have been reported until now in pure chitosan electrospun fiber mats (Jayakumar, Prabaharan, Nair, Tokura, Tamura & Selvamurugan, 2010; Jayakumar, Prabaharan, Sudheesh Kumar, Nair & Tamura, 2011).

The electrospinning technique is very versatile and a wide range of parameters can play an important role in obtaining the desired nanofiber size and microstructure. These parameters include solution viscosity, voltage, feed rate, solution conductivity, capillary-to-collector distance and capillary tube size (Bhardwaj & Kundu; Sill & von Recum, 2008). In this work, a systematic study has been performed in order to solve the aforementioned main problems. By controlling solution parameters a stable process has been achieved allowing obtaining large fiber mats with tailored fiber dimension. Further, the effect of the main processing parameters such as solvent concentration, flow rate, applied voltage, feed rate and inner needle diameter on the chitosan fiber characteristics and sample morphology has been studied in order to set the ground for a systematic and reproducible way to obtain chitosan nanofiber samples for specific applications.

Experimental

Materials

Chitosan practical grade polymer was purchased from Sigma-Aldrich with ≥ 75 % degree of D-acetylation. Dichloromethane (DCM) and Trifluoroacetic acid (TFA, 99 % ReagentPlus) were purchased from Sigma-Aldrich (Table 1). All materials were used as received from the provider.

Table 1 – (Budavari, 1996).

Preparation of the solution

The polymer was dissolved in a TFA/DCM solution with different TFA/DCM volume ratios for a 7 % (weight) of chitosan. The solution were prepared under a constant and vigorous magnetic stirring (JPSelecta, Agimatic-E) at room temperature until complete dissolution of the chitosan. The viscosity of the prepared solutions was measured in a Viscostar Plus set-up from Fungilab. The variation of the viscosity of the polymer solution with varying TFA/DCM ratio is represented in figure 1.

Electrospinning

The polymer solution was placed in a commercial plastic syringe fitted with a steel needle. The inner diameter of the needle was 0.5, 1.0 and 1.7 mm for different experiments. Electrospinning was conducted by applying a voltage ranging from 20 and 30 kV with a PS/FC30P04 power source from Glassman. A syringe pump (Syringepump) fed the polymer solution into the tip at a rate between 1 and 8 $ml.h^{-1}$. The electrospun samples were collected on a grounded collecting plate placed at different distances from 50 to 200 mm from the needle tip.

Characterization

Electrospun fibers were coated with a thin gold layer using a sputter coater from Polaron (SC502) and the morphology of the membranes were observed by scanning electron microscopy (SEM, JSM-6300 from JEOL) at an accelerating voltage of 15 kV. The fiber diameter distribution was calculated over 50 fibers with the Image J software (J, 2011) from the SEM images obtained at a magnification of 3500 x.

144 The degree of deacetylation was determined by nuclear magnetic ressonance (NMR)
145 according to the procedure described in (Fernandez-Megia, Novoa-Carballal, Quiñoá &
146 Riguera, 2005). Five milligram of chitosan after and before electrospun were added to a
147 5 mm NMR tube containing 0.5 mL of 2 % deutorium chloride (DCl, from Fluka)
148 solution in deuterated water (D_2O, Mw=20,02, ACROS Organics) and heated at 70 °C
149 for 1 h in order to speed up the dissolution. The results for the ^{1}NMR were collected in a
150 Varian Unity Plus 300 at 70 ºC.
151
152
153 **Results and Discussion**
154
155 Several parameters affect the fiber morphology and size distribution of the polymer
156 electrospun fibers. Among the most important ones are those corresponding to the initial
157 polymer solution: parameters related to the solvent used (dielectric constant, volatility,
158 boiling point and others), the solution concentration (that controls the viscosity) and the
159 molecular weight of the polymer (that allows polymer entanglement). The main
160 parameters that control the jet formation and solvent evaporation rate are the feed rate
161 through the needle and needle diameter, traveling distance from the needle to the
162 collector, temperature and electric field (Ribeiro, Sencadas, Ribelles & Lanceros-
163 Méndez, 2010; S. Ramakrishna, K. Fujihara, W. E. Teo, T. C. Lim & Ma, 2005; Teo &
164 Ramakrishna, 2006).
165 TFA is a strong acid that can dissolve the polymer through the formation of salts that
166 destroy the strong interactions that exist between the molecules of chitosan (Ohkawa,
167 Cha, Kim, Nishida & Yamamoto, 2004). The salt formation occurs between the TFA
168 and the amino groups along the chitosan chain after the following sequential steps: first,

169 protonation of amine groups (-NH_2) along the chain of chitosan; second, ionic
170 interaction between protonated amino groups (-NH_3) and then formation of
171 trifluoroacetate anions. In this configuration, the salts are soluble in an aqueous media.
172 In this work, solutions of chitosan in TFA/DCM with different relative concentrations
173 were used in order to taylor viscosity and conductivity of the solvent. These parameters
174 have strong influence in the electrospinning process and therefore in the final fiber
175 morphology. The SEM images for the electrospun samples obtained from a solution of
176 chitosan with different TFA/DCM volume ratios and fixed traveling distance of 150
177 mm, needle diameter of 0.5 mm, flow rate of 2 $ml.h^{-1}$ and a voltage of 25 kV are
178 presented in Figure 2.
179 Schiffman et al. reported that electropinning of chitosan in pure TFA solvent was viable
180 for lower chitosan concentrations (2.7 % (w/v)) (Schiffman & Schauer, 2006). In the
181 present work, it was dificult to stabilize the electrospinning process for TFA/DCM
182 concentrations rich in TFA solvent (higher than 80 % TFA) in the solution due to the
183 presence of sparks that frequently appeared during the fiber processing, even for small
184 applied electric fileds, therefore hindering the electrospinning process. An increase of
185 TFA in the solution increases the viscosity (figure 1) and the conductivity of the
186 medium, which are at the origin of the sparks. Electrospinning involves stretching of the
187 solution caused by the repulsion of the charges at its surface. If the conductivity of the
188 solution is increased, more charges can be carried out by the electrospinning jet. The
189 free amines trifluoroacetate anions formed during the chitosan dissolution in TFA
190 increase the conductivity of the solution (Dannhauser & Cole, 1952) and, therefore, the
191 critical voltage for electrospinning to occur is reduced.
192 Further, for TFA/DCM solvent mixtures with low TFA content, the dissolution of the
193 polymer was extremely dificult and during the electrospinning process some drops

194 falled from the needle due to the lower viscosity of the solution, These drops complety
195 dissolved the formed fiber and destroyed the homogenety of the electrospun mats. It
196 was also observed that the average fiber diameter of the electrospun mats decreased
197 with increasing DCM content in the solvent mixture. On the other hand, a larger fiber
198 size distribution was observed with increasing TFA content in the solution a (Figure 3).
199 Figure 3 was obtained from histograms analogous to those shown in Figure 2 (the ones
200 corresponding to Figures 2c and 2d are included in Figure 3), from which the mean
201 value was calculated. The bars in Figure 3 indicate the average and the standard
202 deviation of the fiber diameters.
203 The influence of the inner diameter of the needle in the average size of the electrospun
204 fibers was characterized. For the samples processed with a needle with an inner
205 diameter of 0.5 mm, the presence of very thin fibers with diameters ~ 250 nm was
206 observed. This fact can be attributed to the lower DCM solvent evaporation temperature
207 (Figure 4). On the other hand, the samples obtained with a higher needle diameter show
208 a more uniform fiber size distribution. It was also noted that all samples were free of
209 beads, indicating that the tested chitosan electrospinnig conditions provide sufficient
210 chain entanglement for fiber formation.
211 The presence of small particles (Figure 4b) on the surface of the electrospun fibers has
212 been explained by Zhang et al. as a consequence of the presence of salts (Zhang, Yuan,
213 Wu, Han & Sheng, 2005) originated by the chitosan dissolution in the TFA acid, as
214 explained above. These salts are commonly observed for higher polymer concentrations
215 and higher TFA content in the chitosan-TFA/DCM solvent solution.
216 The average size of the fibers for the different needle inner diameters was calculated
217 and the results show a slight increase of the average fiber diameter from ~ 360 to 410
218 nm with increasing inner needle diameter (figure 5).

219 The fiber diameter distribution along the sample is quite similar for all the electrospun
220 samples, being therefore independent of the needle inner diameter. Literature shows
221 contradictory results in this point. Macossay et al. found no influence of the needle
222 diameter on the average fiber diameter of poly(methyl methacrylate) electrospun fibers
223 (Macossay, Marruffo, Rincon, Eubanks & Kuang, 2007), while Katti et al. and Ribeiro
224 et al. reported that the fiber diameter decreases with decreasing needle inner diameter
225 (Katti, Robinson, Ko & Laurencin, 2004; Ribeiro, Sencadas, Ribelles & Lanceros-
226 Méndez, 2010).
227 A decrease of the inner diameter of the needle causes a reduction of the droplet at the tip
228 and therefore the surface tension of the droplet increases. Then, for a given applied
229 voltage, a larger Coulombic force is required to cause the jet initiation, which results in
230 a decrease of the jet acceleration and, as a consequence, more time is required for the
231 solution to be stretched and elongated before it is collected (S. Ramakrishna, K.
232 Fujihara, W. E. Teo, T. C. Lim & Ma, 2005).
233 The influence of the distance between the needle tip to the grounded collector on the
234 fiber average diameter and distribution was also analyzed. It was observed that the
235 fibers with the smallest average diameter, ~260 nm, were obtained for the samples with
236 a 50 mm distance between needle tip and collector and that the mean fiber diameter
237 increases by increasing the distance between the needle tip and the collector. A
238 maximum average fiber diameter of ~ 500 nm was obtained for a traveling distance of
239 200 mm (Figure 6).
240 It was also observed that the mean diameter fiber distribution increases with increasing
241 the distance between needle tip and sample collector. The presence of sub-structures of
242 smaller fibers between the smooth large fibers (Figure 7) suggests the formation of a
243 secondary jet during the main electrospinning process due to the high solution viscosity

(Figure 1). Ding et al. (Ding & et al., 2006) pointed out that this fact is related to certain processing conditions such as high voltage, low relative humidity and fast phase separation of polymer and solvent during the flight between the needle and the collector.

Ramakrishna et al. (S. Ramakrishna, K. Fujihara, W. E. Teo, T. C. Lim & Ma, 2005) justified these structures as a consequence of the formations and ejection of smaller jets from the surface of the primary jets, which is comparable to the ejection of the initial jet from the surface of a charged droplet. It was proposed that the elongation of the jet and evaporation of the solvent modifies the shape and the charge density of the jet during the traveling between the tip and the collector. Thus, the balance between the electrical forces and surface tension can change, giving rise to instabilities in the shape of the jet. Such instabilities can decrease the local charge per unit surface area by ejecting a smaller jet from the surface of the primary jet or by splitting apart into two smaller jets. In this work a blend of two solvents with different boiling points (Table 1) has been used and the observed sub-structures of smaller fibers can be related to the fast evaporation of the DCM solvent from the blend during the traveling from the needle tip to the collector, leaving behind solidified fibers with smaller diameters than the ones that crystallize later when the TFA solvent evaporates. This phenomenon was also observed in Figures 2 and 3, when the effect of TFA/DCM solvent ratio on fiber diameter and mat morphology was presented.

It is pointed out that an increase of the distance between the tip and the collector often results in a decrease of the fiber diameter (S. Ramakrishna, K. Fujihara, W. E. Teo, T. C. Lim & Ma, 2005). However, in the present work it was observed that the diameter of the fibers increases for increasing distance between the needle tip and the grounded collector. This behavior is to be ascribed to the decrease of the electrostatic field

strength resulting in a decrease of the electrostatic force and therefore on the stretching of the fibers.

Tip to collector distance has a direct influence on the jet flight time and electric field strength: a decrease of the distance shortens flight and solvent evaporation times and increases the electric field strength. A decrease in the tip-collector distance has a similar effect as increasing the voltage (Figure 8).

The changes in the applied electric field have strong influence on the shape of the droplet at the needle tip, its surface charge, dripping rate, velocity of the flowing fluid and hence on the fiber structure and morphology. Similarly, the needle tip to collector distance also determines the time available for fiber drying and the space available for fiber splaying and whipping to take place.

The high voltage will induce the necessary charge distribution on the solution and initiate the electrospinning process when the electrostatic force overcomes the surface tension of the solution (S. Ramakrishna, K. Fujihara, W. E. Teo, T. C. Lim & Ma, 2005). For higher electric fields, the jet will accelerate and stretch due to the larger Coulombic forces, which results in a reduction of the fiber average diameter and also promotes faster solvent evaporation to yield drier fibers (S. Ramakrishna, K. Fujihara, W. E. Teo, T. C. Lim & Ma, 2005).

Finally, the influence of the feed rate on the average fiber distribution was characterized (Figure 9). A minimum value of solution volume suspended at the end of the needle should be maintained in order to form a stable Taylor cone (Teo & Ramakrishna, 2006). The feed rate determines the amount of solution available for the electrospining process. Typically, when the feed rate increases, a corresponding increase of the fiber diameter is observed, as observed i.e. for poly(vinylidene fluoride) (Ribeiro, Sencadas, Ribelles & Lanceros-Méndez, 2010) and for poly(L-lactide acid) (Clarisse & et al., 2011). In

chitosan such behavior was not found and the fiber diameter distribution is quite similar for the different feed rates within the range studied in the present work (Figure 9).

It was expected that increasing feed rate will increase the volume of the solution drawn from the needle tip, and consequently the jet would take a longer time to dry. The lower boiling point of the solvents used in this work (Table 1) allows the fast evaporation during the flight time. In this situation, full solvent evaporation has already occurred when the fiber reaches the grounded collector and therefore the feed rate does not have influence on the fiber diameter.

Most of the physical and chemical properties of this biopolymer strongly depend on the degree of deacetylation (DD) (Lavertu et al., 2003). The DD can be calculated from the ^{1}NMR spectra (figure 10) through:

$$DD(\%) = \frac{H_1 D}{H_1 D + \left(\frac{H_{ac}}{3}\right)} \times 100$$

where H_1D is the peak corresponding to the H_1 proton of the deacetylated monomer (duplet at δ= 4.858 ppm) and H_{ac} is the peak of the three protons of the acetyl group (singlet at δ= 1.988 ppm) (Lavertu et al., 2003). The obtained results show that the commercial chitosan has a DD of 78 %, which is similar to the value given by the producer and also similar to the values obtained for the electrospun fibers. It is therefore concluded that the electrospinning process does not affect the degree of deacetylation of the polymer.

Conclusions

Large chitosan mats with uniform fibers of submicron diameters without beads have been prepared from trifluoroacetic acid / dichloromethane mixture solutions by a stable electrospinnig process. It was observed that an increase of the DCM present in the solvent blend solution produces nanofibers with smaller diameters and narrower diameter distribution. Inclusion of DCM within the TFA solutions modifies solution viscosity and electrical characteristics, leading to a stable flow rate and avoiding spark formation. The inner diameter of the needle and the feed rate does not have influence in the chitosan electrospun fiber diameter. On the other hand, it was observed that a decrease of the distance from the needle tip to the grounded collector gives origin to nanofibers with smaller diameters. Finally, an increase of the applied voltage also decreases the nanofibers diameter. The degree of deacetylation of the polymer is not affected by the electrospinning process.

Acknowledgements

This work is funded by FEDER funds through the "Programa Operacional Factores de Competitividade – COMPETE" and by national funds by FCT- Fundação para a Ciência e a Tecnologia, project references NANO/NMed-SD/0156/2007. V.S. thanks the FCT for the SFRH/BPD/63148/2009 grants. JLGR acknowledge the support of the Spanish Ministry of Science and Innovation through project No. MAT2010-21611-C03-01 (including the FEDER financial support) and Programa Nacional de Internacionalización de la I+D project EUI2008-00126. Funding for research in the field of Regenerative Medicine through the collaboration agreement from the Conselleria de Sanidad (Generalitat Valenciana), and the Instituto de Salud Carlos III (Ministry of Science and Innovation) is also acknowledged.

Thanks are due to the National NMR Network that was purchased within the framework of the National Program for Scientific Re-equipment, contract REDE/1517/RMN/2005 with funds from POCI 2010 (FEDER) and FCT. Also thank to the UPV Microscopy Service for the use of their lab.

References

Baldrick, P. (2010). The safety of chitosan as a pharmaceutical excipient. *Regulatory Toxicology and Pharmacology, 56*(3), 290-299.

Beachley, V., & Wen, X. (2010). Polymer nanofibrous structures: Fabrication, biofunctionalization, and cell interactions. *Progress in Polymer Science, 35*(7), 868-892.

Bhardwaj, N., & Kundu, S. C. Electrospinning: A fascinating fiber fabrication technique. *Biotechnology Advances, 28*(3), 325-347.

Budavari, S. (1996). *An Encyclopedia of Chemicals, Drugs, and Biologicals*. New Jersey: Merck & Co.

Clarisse, R., & et al. (2011). Tailoring the morphology and crystallinity of poly(L-lactide acid) electrospun membranes. *Science and Technology of Advanced Materials, 12*(1), 015001.

Dannhauser, W., & Cole, R. H. (1952). On the Dielectric Constant of Trifluoroacetic Acid1. *Journal of the American Chemical Society, 74*(23), 6105-6105.

Ding, B., & et al. (2006). Formation of novel 2D polymer nanowebs via electrospinning. *Nanotechnology, 17*(15), 3685.

Fernandez-Megia, E., Novoa-Carballal, R., Quiñoá, E., & Riguera, R. (2005). Optimal routine conditions for the determination of the degree of acetylation of chitosan by 1H-NMR. *Carbohydrate Polymers, 61*(2), 155-161.

Honarkar, H., & Barikani, M. (2009). Applications of biopolymers I: chitosan. *Monatshefte Fur Chemie, 140*(12), 1403-1420.

J, I. (2011). Image Processing and Analysis in Java available from http://rsbweb.nih.gov/ij/index.html.

Jayakumar, R., Menon, D., Manzoor, K., Nair, S. V., & Tamura, H. (2010). Biomedical applications of chitin and chitosan based nanomaterials--A short review. *Carbohydrate Polymers, 82*(2), 227-232.

Jayakumar, R., Prabaharan, M., Nair, S. V., & Tamura, H. Novel chitin and chitosan nanofibers in biomedical applications. *Biotechnology Advances, 28*(1), 142-150.

Jayakumar, R., Prabaharan, M., Nair, S. V., Tokura, S., Tamura, H., & Selvamurugan, N. (2010). Novel carboxymethyl derivatives of chitin and chitosan materials and their biomedical applications. *Progress in Materials Science, 55*(7), 675-709.

Jayakumar, R., Prabaharan, M., Sudheesh Kumar, P. T., Nair, S. V., & Tamura, H. (2011). Biomaterials based on chitin and chitosan in wound dressing applications. *Biotechnology Advances, 29*(3), 322-337.

Katti, D. S., Robinson, K. W., Ko, F. K., & Laurencin, C. T. (2004). Bioresorbable nanofiber-based systems for wound healing and drug delivery: Optimization of fabrication parameters. *Journal of Biomedical Materials Research Part B: Applied Biomaterials, 70B*(2), 286-296.

Krajewska, B. (2005). Membrane-based processes performed with use of chitin/chitosan materials. *Separation and Purification Technology, 41*(3), 305-312.

Lavertu, M., Xia, Z., Serreqi, A. N., Berrada, M., Rodrigues, A., Wang, D., Buschmann, M. D., & Gupta, A. (2003). A validated 1H NMR method for the determination of the degree of deacetylation of chitosan. *Journal of Pharmaceutical and Biomedical Analysis, 32*(6), 1149-1158.

392 Macossay, J., Marruffo, A., Rincon, R., Eubanks, T., & Kuang, A. (2007). Effect of
393 needle diameter on nanofiber diameter and thermal properties of electrospun
394 poly(methyl methacrylate). *Polymers for Advanced Technologies, 18*(3), 180-183.
395 Malafaya, P. B., Silva, G. A., & Reis, R. L. (2007). Natural-origin polymers as carriers
396 and scaffolds for biomolecules and cell delivery in tissue engineering applications.
397 *Advanced Drug Delivery Reviews, 59*(4-5), 207-233.
398 Ohkawa, K., Cha, D., Kim, H., Nishida, A., & Yamamoto, H. (2004). Electrospinning
399 of Chitosan. *Macromolecular Rapid Communications, 25*(18), 1600-1605.
400 Pillai, C. K. S., Paul, W., & Sharma, C. P. (2009). Chitin and chitosan polymers:
401 Chemistry, solubility and fiber formation. *Progress in Polymer Science, 34*(7), 641-678.
402 Ravi Kumar, M. N. V. (2000). A review of chitin and chitosan applications. *Reactive*
403 *and Functional Polymers, 46*(1), 1-27.
404 Ribeiro, C., Sencadas, V., Ribelles, J. L. G., & Lanceros-Méndez, S. (2010). Influence
405 of Processing Conditions on Polymorphism and Nanofiber Morphology of Electroactive
406 Poly(vinylidene fluoride) Electrospun Membranes. *Soft Materials, 8*(3), 274 - 287.
407 S. Ramakrishna, K. Fujihara, W. E. Teo, T. C. Lim, & Ma, Z. (2005). *Introduction to*
408 *electrospinning and nanofibers*. Singapure: World Scientific.
409 Schiffman, J. D., & Schauer, C. L. (2006). Cross-Linking Chitosan Nanofibers.
410 *Biomacromolecules, 8*(2), 594-601.
411 Schiffman, J. D., & Schauer, C. L. (2007). One-Step Electrospinning of Cross-Linked
412 Chitosan Fibers. *Biomacromolecules, 8*(9), 2665-2667.
413 Sill, T. J., & von Recum, H. A. (2008). Electrospinning: Applications in drug delivery
414 and tissue engineering. *Biomaterials, 29*(13), 1989-2006.
415 Teo, W. E., & Ramakrishna, S. (2006). A review on electrospinning design and
416 nanofibre assemblies. *Nanotechnology, 17*(14), R89.

417 Yaghobi, N., & Hormozi, F. (2010). Multistage deacetylation of chitin: Kinetics study.
418 *Carbohydrate Polymers, 81*(4), 892-896.
419 Zhang, C., Yuan, X., Wu, L., Han, Y., & Sheng, J. (2005). Study on morphology of
420 electrospun poly(vinyl alcohol) mats. *European Polymer Journal, 41*(3), 423-432.

421

Figure 1 – Variation of the viscosity of the polymer solution with varying TFA/DCM ratio. The line is just a guide for the eyes.

Figure 2 – Morphology of the chitosan mats for the samples obtained with a 7 % (w/v) polymer solution at a traveling distance of 150 mm, needle diameter of 0.5 mm, flow rate of 2 $ml.h^{-1}$ and a voltage of 25 kV: a) 80:20 and b) 60:40 TFA/DCM (v/v) solution; c) and d) represent the fiber diameter histograms of the corresponding figures.

Figure 3 – Influence of the TFA/DCM volume ratio in the distribution of fiber diameters in the electrospun mats obtained for a 7 % (w/v) chitosan solution at a fixed traveling distance of 150 mm, needle diameter of 0.5 mm, flow rate of 2 $ml.h^{-1}$ and a voltage of 25 kV.

Figure 4 – Morphology of the chitosan mats for the samples obtained for a 7 % (w/v) polymer solution, a 70/30 TFA/DCM solvent solution, a traveling distance of 150 mm, flow rate of 2 $ml.h^{-1}$ and a voltage of 25 kV for needle inner diameters of a) 0.5 mm and b) 1.7 mm; c) and d) represent the fiber diameter histograms of the corresponding figures.

Figure 5 – Influence of the inner diameter of the needle in the average fiber diameter and distribution for the electrospun mats obtained for a 7 % (w/v) chitosan solution, a 70/30 TFA/DCM solvent solution, a traveling distance of 150 mm, flow rate of 2 $ml.h^{-1}$ and a voltage of 25 kV.

Figure 6 – Influence of the traveling distance on the fiber average diameter and distribution in the electrospun mats obtained for a 7 % (w/v) chitosan solution, a 70/30 TFA/DCM solvent solution, a needle inner diameter of 0.5 mm, a flow rate of 2 $ml.h^{-1}$ and a voltage of 25 kV.

453

454 **Figure 7 –** Morphology of the chitosan mats for the samples obtained for a 7 % (w/v)
455 polymer solution, a 70/30 TFA/DCM solvent solution and a needle diameter of 0.5 mm,
456 at a traveling distance of 150 mm, flow rate of 2 $ml.h^{-1}$ a voltage of 25 kV and a
457 distance between the needle tip to the sample collector of a) 50 mm and b) 200 mm.
458

459

460 **Figure 8 –** Influence of the applied voltage on fiber average diameter and distribution in
461 the electrospun mats obtained for a 7 % (w/v) chitosan solution, a 70/30 TFA/DCM
462 solvent solution, needle inner diameter of 1.7 mm, flow rate of 2 $ml.h^{-1}$ and a traveling
463 distance of 15 cm.
464

465 **Figure 9 –** Influence of the feed rate on the average fiber diameter and distribution of
466 the electrospun mats obtained for a 7 % (w/v) chitosan solution, a 70/30 TFA/DCM
467 solvent solution, needle inner diameter of 0.5 mm, flow rate of 2 $ml.h^{-1}$, a traveling
468 distance of 15 cm and a 25 kV applied voltage.
469

470 **Figure 10 –** ^{1}H-NMR spectra of electrospun chitosan nanofibers at 70 °C.
471

472 **Table 1** – Properties of the solvents used in the present work [17].
473

474

474

475

476 Table 1

Solvent	Melting Point	Boiling Point	Density	Dipole Moment	Dielectric Constant
	ºC	ºC	$g.cm^{-3}$	Debye	
TFA	-15.2	73.0	1.535	2.28	8.42
DCM	-95.1	40.0	1.327	1.60	8.93

477

478

479

479

480 Figure 1

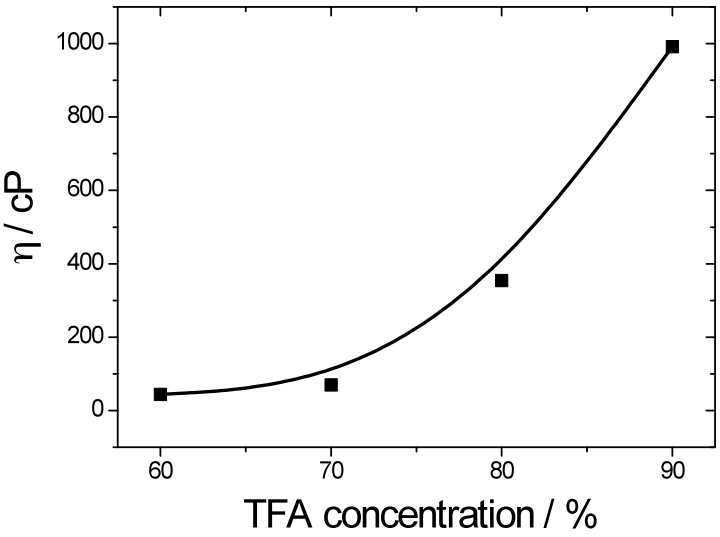

481

482

Figure 2

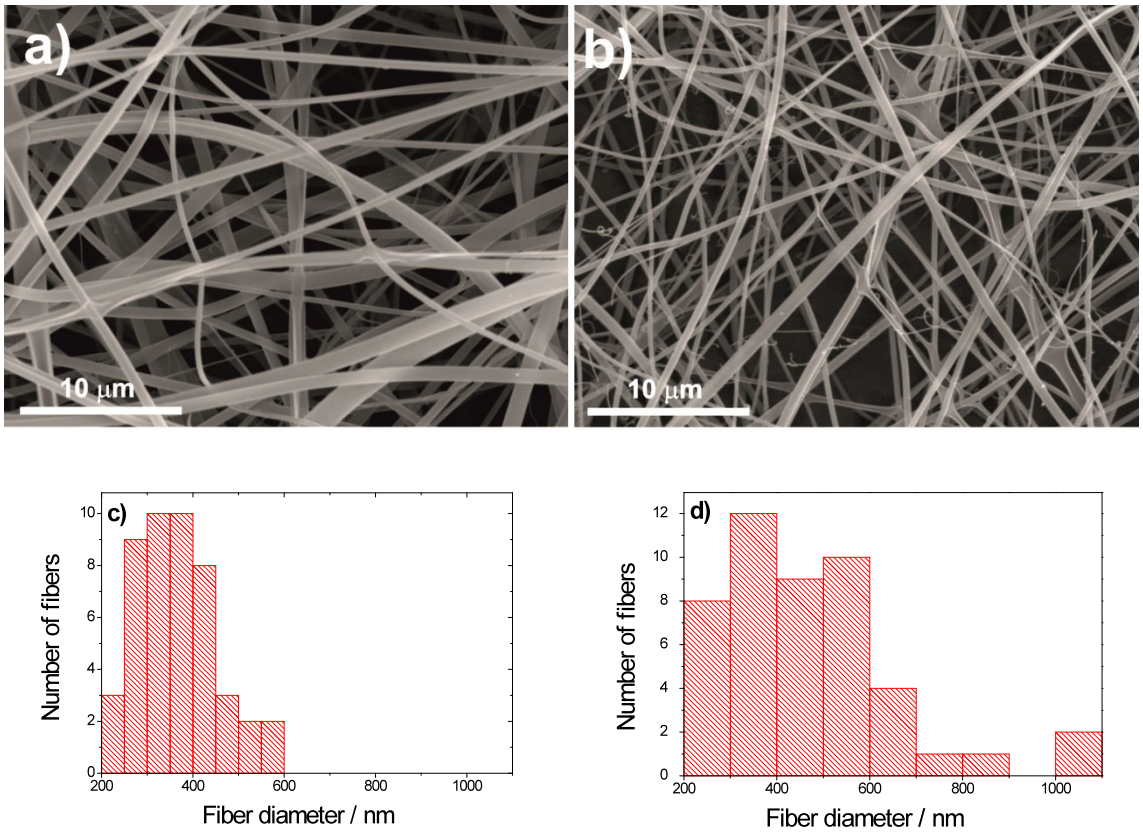
a)
10 μm
b)
10 μm
c)
Number of fibers
Fiber diameter / nm
d)
Number of fibers
Fiber diameter / nm

Figure 3

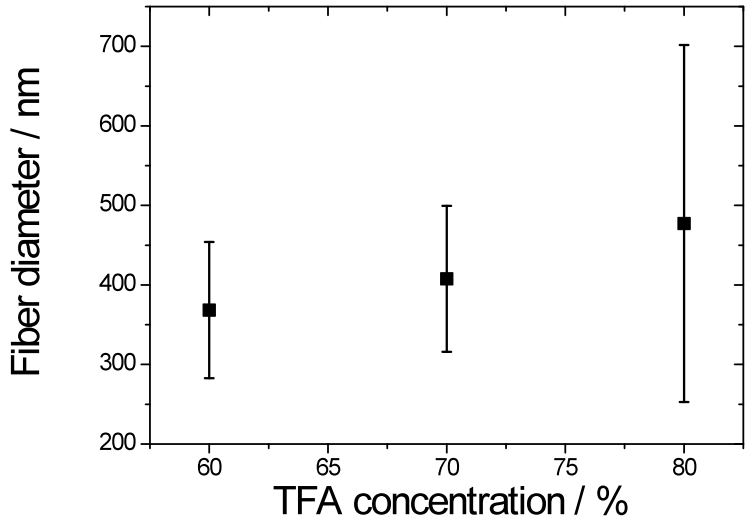
Fiber diameter / nm
700
600
500
400
300
200
60
65
70
75
80
TFA concentration / %

489

490 Figure 4

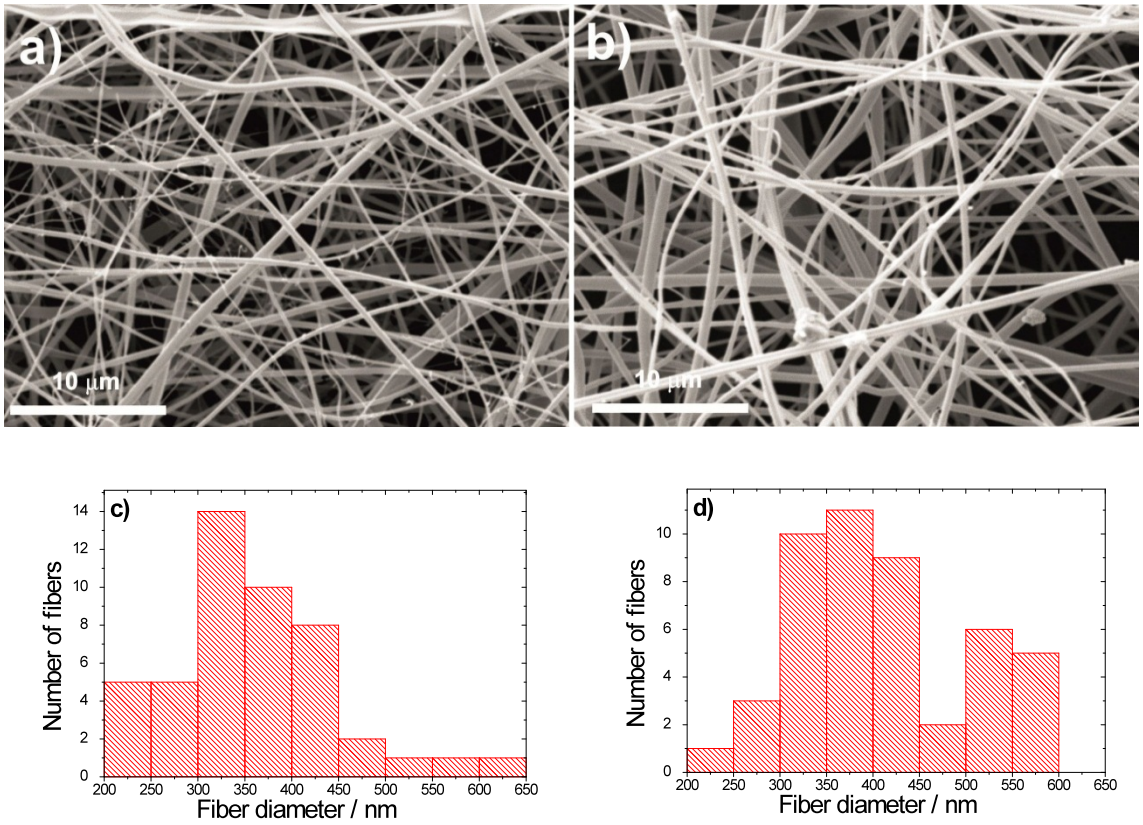

491

492

492

493 Figure 5

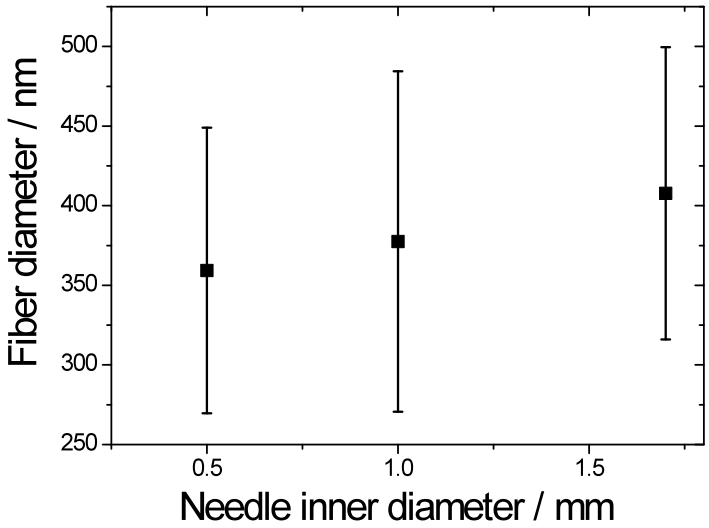

494

495

Figure 6

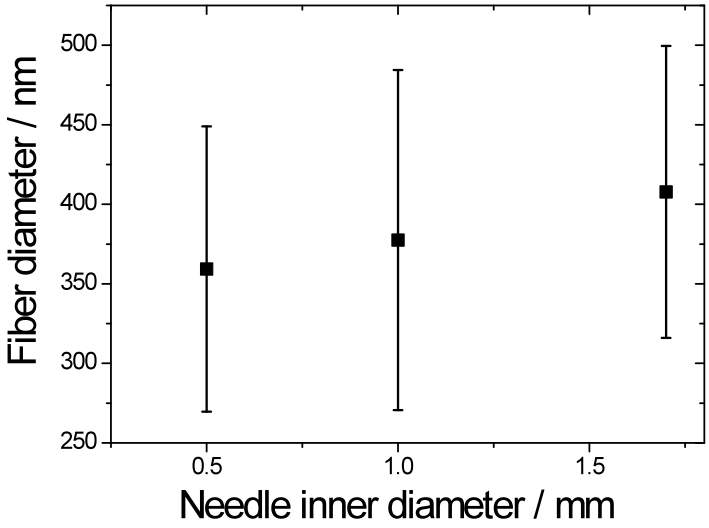
Fiber diameter / nm
500
450
400
350
300
250
0.5
1.0
1.5
Needle inner diameter / mm

499

500 Figure 7

501

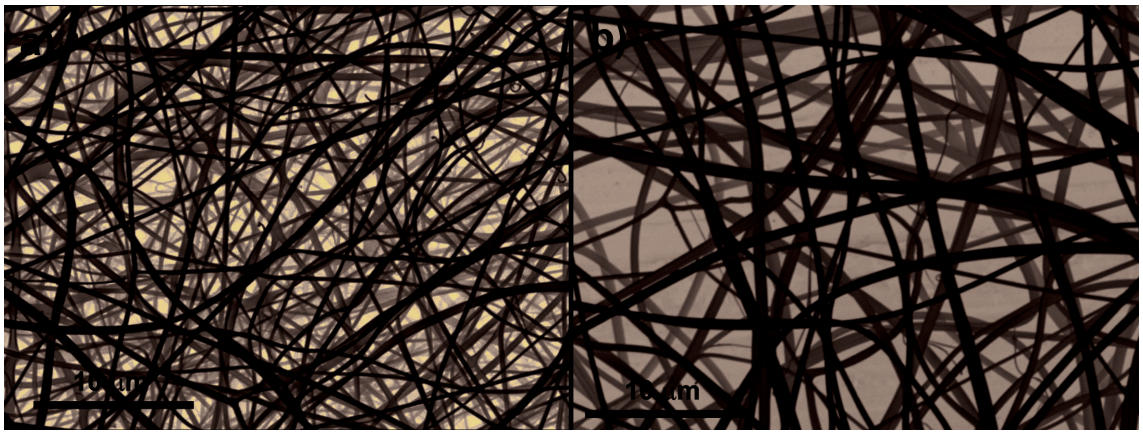

502

503

503

504 Figure 8

505

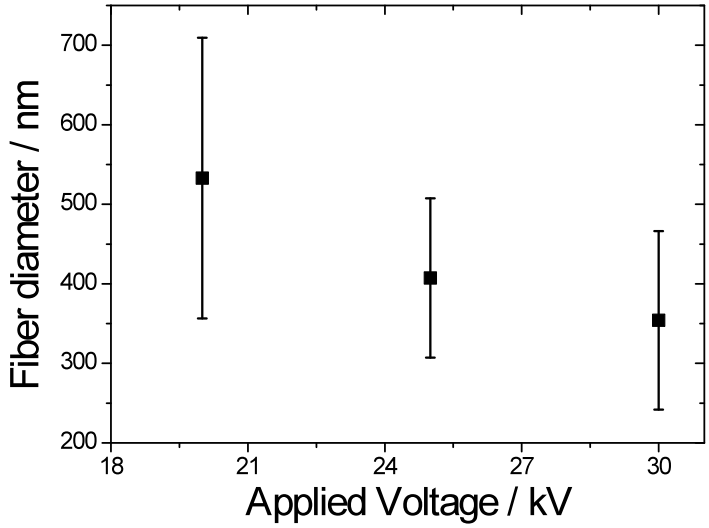

506

507

507

508 Figure 9

509

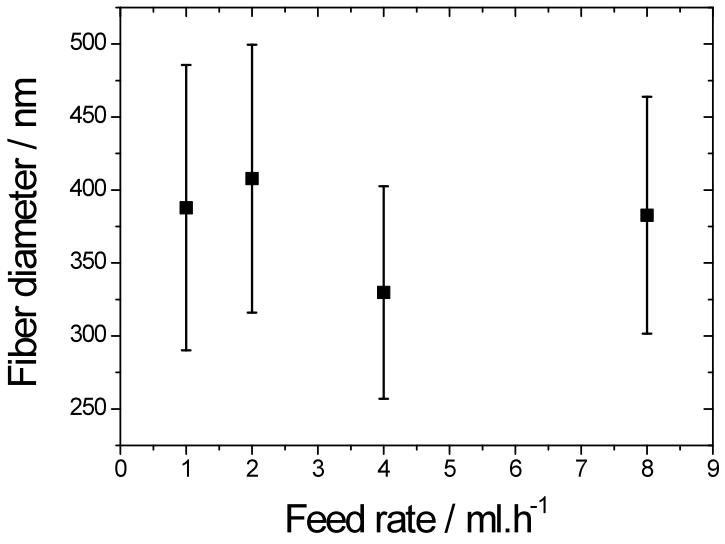

510

511

511

512 Figure 10

513

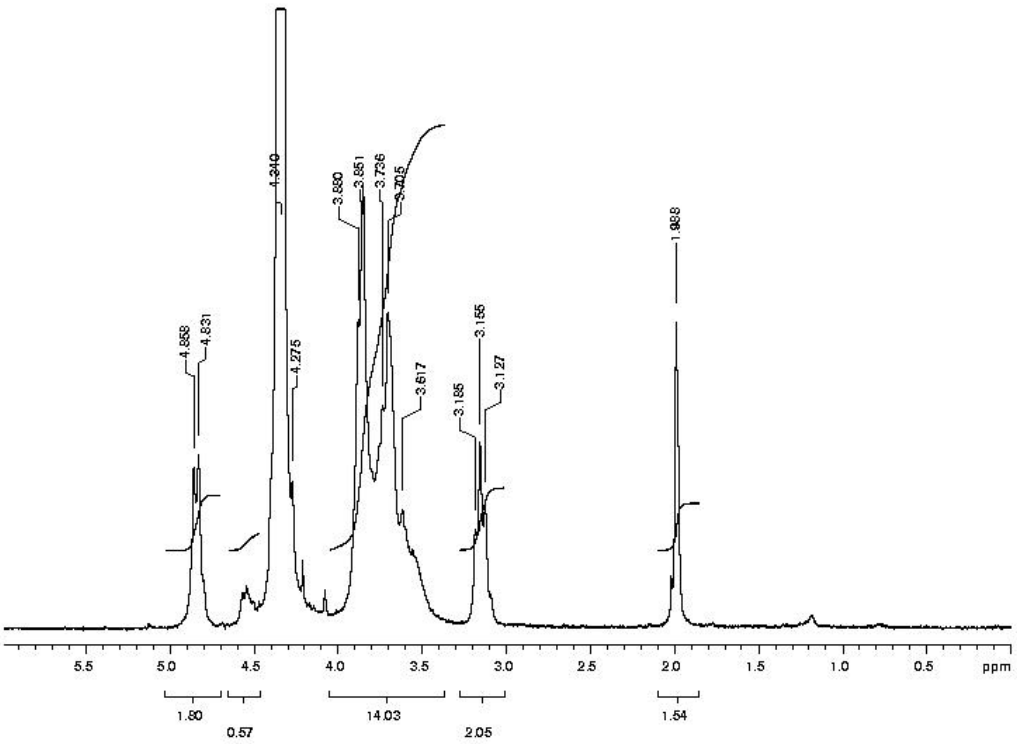

514

515